CHEMISTRY
A EUROPEAN JOURNAL

DOI: 10.1002/chem.201000524

Formation of the Distinct Redox-Interrelated Forms of Nitric Oxide from Reaction of Dinitrosyl Iron Complexes (DNICs) and Substitution Ligands

Tsai-Te Lu, Chih-Hao Chen, and Wen-Feng Liaw*[a]

Abstract: Release of the distinct NO redox-interrelated forms (NO^+, $^{\bullet}NO$, and HNO/NO^-), derived from reaction of the dinitrosyl iron complex (DNIC) $[(NO)_2Fe(C_{12}H_8N)_2]^-$ (**1**) ($C_{12}H_8N$ = carbazolate) and the substitution ligands $(S_2CNMe_2)_2$, $[SC_6H_4$-*o*-$NHC(O)(C_5H_4N)]_2$ ($(PyPepS)_2$), and $P(C_6H_3$-3-$SiMe_3$-2-$SH)_3$ ($[P(SH)_3]$), respectively, was demonstrated. In contrast to the reaction of $(PyPepS)_2$ and DNIC **1** in a 1:1 stoichiometry that induces the release of an NO radical and the formation of complex $[PPN][Fe(PyPepS)_2]$ (**4**), the incoming substitution ligand $(S_2CNMe_2)_2$ triggered the transformation of DNIC **1** into complex $[(NO)Fe(S_2CNMe_2)_2]$ (**2**) along with *N*-nitrosocarbazole (**3**). The subsequent nitrosation of *N*-acetylpenicillamine (NAP) by *N*-nitrosocarbazole (**3**) to produce *S*-nitroso-*N*-acetylpenicillamine (SNAP) may signify the possible formation pathway of *S*-nitrosothiols from DNICs by means of transnitrosation of *N*-nitrosamines. Protonation of DNIC **1** by $[P(SH)_3]$ triggers the release of HNO and the generation of complex $[PPN][Fe(NO)P(C_6H_3$-3-$SiMe_3$-2-$S)_3]$ (**5**). In a similar fashion, the nucleophilic attack of the chelating ligand $P(C_6H_3$-3-$SiMe_3$-2-$SNa)_3$ ($[P(SNa)_3]$) on DNIC **1** resulted in the direct release of $[NO]^-$ captured by $[(^{15}NO)Fe(SPh)_3]^-$, thus leading to $[(^{15}NO)(^{14}NO)Fe(SPh)_2]^-$. These results illustrate one aspect of how the incoming substitution ligands ($(S_2CNMe_2)_2$ vs. $(PyPepS)_2$ vs. $[P(SH)_3]/[P(SNa)_3]$) in cooperation with the carbazolate-coordinated ligands of DNIC **1** function to control the release of NO^+, $^{\bullet}NO$, or $[NO]^-$ from DNIC **1** upon reaction of complex **1** and the substitution ligands. Also, these results signify that DNICs may act as an intermediary of NO in the redox signaling processes by providing the distinct redox-interrelated forms of NO to interact with different NO-responsive targets in biological systems.

Keywords: bioinorganic chemistry · iron · ligand effects · nitric oxide · redox chemistry

Introduction

Nitric oxide, stored by the potential redox-interrelated forms NO^+, $^{\bullet}NO$, and NO^-, has been known to participate in diverse physiological processes through interaction with various NO-responsive targets within proteins.[1] In contrast to inducing apoptosis through activation of caspase activity in thymocytes and neuronal cells that contain low nonheme iron levels, NO inhibits cell death by blocking caspase activity by means of S-nitrosation of the cysteine within the active site of the enzyme in hepatocytes and endothelial cells, a cell type with high nonheme iron content.[2] Glutathione (GSH) reductase that catalyzes the nicotinamide adenine dinucleotide phosphate (NADPH)-dependent reduction of the oxidized glutathione (GSSG) to maintain the intracellular level of GSH is inhibited upon nitrosation of its His467 of the catalytic site.[3] Compared to S-nitrosation of the soluble guanylate cyclase (sGC) that contributes to the dysfunction of vascular NO/cyclic guanosine monophosphate (cGMP) signaling, nitric oxide binds to the regulatory ferrous heme group bound to His105 of sGC to stimulate cGMP formation and lead to vasodilation.[4] Obviously, the paradox, the versatile response of NO-sensing proteins to $NO^+/^{\bullet}NO$, demonstrates that the redox-interrelated forms ($NO^+/^{\bullet}NO$) of nitric oxide recognize the target to trigger varieties of signaling transduction. Also, nonheme iron centers (i.e., [Fe–S] clusters) play sensory and regulatory roles in transducing the NO signal to modulate cellular iron homeostasis and alter the metabolism of bacteria.[5,6] In addition, nitroxyl (HNO), which converts rapidly to N_2O in aqueous solution, undergoes addition to protein thiols to result in

[a] Dr. T.-T. Lu, C.-H. Chen, Prof. Dr. W.-F. Liaw
Department of Chemistry, National Tsing Hua University
Hsinchu 30013 (Taiwan)
Fax: (+886) 3-5711082
E-mail: wfliaw@mx.nthu.edu.tw

Supporting information for this article is available on the WWW under http://dx.doi.org/10.1002/chem.201000524.

sulfhydryl oxidation through the proposed N-hydroxysulfenamide intermediate RSNHOH.[7]

S-nitrosation has emerged as a post-translational modification of proteins by covalent attachment of a nitroso group to the thiol side chain of cysteine to convey part of the ubiquitous influence of nitric oxide on cellular signal transduction.[8] NO is known to transform into N_2O_3 and $ONOO^-$ under the presence of O_2 or O_2^-, respectively, to nitrosate cysteine, thus leading to the formation of *S*-nitrosothiol.[9] Also, *S*-nitrosothiol, *N*-nitrosamine, and heme-NO display an S-nitrosation ability.[10] Dinitrosyl iron complexes (DNICs) with a typical EPR signal at $g=2.03$ are known as another type of naturally occurring forms for storage and transport of NO in biological systems.[11] De novo synthesis of *S*-nitrosothiol in an O_2-independent pathway is proposed to result from transnitrosation of DNICs derived from nitrosylation of cellular labile iron pool.[12a] S-nitrosation of Cys34 of bovine serum albumin by DNIC was reported upon treatment of bovine serum albumin with DNIC–Cys.[12b] Studies on the presence or absence of glutathione that regulates DNIC to stimulate cGMP formation by means of heme nitrosylation or to inactivate sGC through S-nitrosation were also reported.[4a] In particular, it is proposed that DNICs may nitrosate proteins more selectively than NO_x because accessibility to DNIC is determined by the three-dimensional structure of the protein in the immediate vicinity of the target site.[3]

In chemistry, one feature of metal nitrosyl complexes is the "redox-noninnocent" nature of the NO ligand that regulates NO reactivity and the electronic structure of the $\{M(NO)_x\}$ (M = transition metal) core. It is, however, complicated to define the "noninnocent" character of NO acting as NO^+, NO^-, or $^{\bullet}NO$ within the class of $\{Fe(NO)_2\}^9$ DNICs.[13] The binding of NO to the varieties of transition metals that exist as $\{M–NO^+\}$, $\{M–NO^{\bullet}\}$, and $\{M–NO^-\}$ has been intensely studied. Isolation of $[IrCl_4(CH_3CN)N(O)SCH_2Ph]^-$ obtained from reaction of $[IrCl_5NO]^-$ and $HSCH_2Ph$ implies that nucleophilic attack of thiolate on the nitrosyl ligand leads to the transformation of an Ir–NO complex into [Ir–N(O)SR].[14] Hydride reduction of the nitrosyl ligand of the $\{Ru(NO)\}^6$ [Ru(ttp)(NO)(1-MeIm)]$^+$ (ttp = tetratolylporphyrinato dianion, Im = imidazole) produces the Ru-bound HNO.[15] Also, nitric oxide is converted to HNO by means of a proton-coupled electron-transfer reaction upon the nitrosylation of $[HCr(CO)_3C_5Me_5]$.[16] We also noticed that protonation of the reduced species of $\{Fe(NO)\}^7$, in the Enemark–Feltham electronic notation, [Fe(tpp)(NO)] (tpp = tetraphenylporphyrinato dianion) by phenol yields the proposed [Fe(tpp)(HNO)].[17] In particular, the free $^{\bullet}NO$ release from the dimeric DNICs (Roussin's red esters) under photolysis was reported.[18] In our previous study, the NO-releasing ability of $\{Fe(NO)_2\}^9$ DNICs regulated by the R group of the thiolate-coordinated ligands was demonstrated.[19] Recently, the oxidation state of the NO ligand of DNICs going from $^{\bullet}NO$ to NO^- finely tuned by the ligation mode of DNICs was also concluded.[20] In this contribution, in addition to the oxidation state of the intrinsic NO ligand of DNICs regulated by the coordinated ligands,[19,20] the release of the distinct NO redox-interrelated forms, namely, *N*-nitrosocarbazole, $^{\bullet}NO$, and HNO/NO^-, derived from DNIC $[(NO)_2Fe(C_{12}H_8N)_2]^-$ (**1**) ($C_{12}H_8N$ = carbazolate) modulated by the incoming substitution ligands $(S_2CNMe_2)_2$, $(PyPepS)_2$, and $P(C_6H_3\text{-}3\text{-}SiMe_3\text{-}2\text{-}SH)_3$, respectively, was demonstrated. In particular, the intramolecular N-nitrosation of the coordinated carbazolate (a tryptophan (Trp) analogue) ligand of DNIC **1** to yield *N*-nitrosocarbazole and the subsequent nitrosation of *N*-acetylpenicillamine (NAP) by *N*-nitrosocarbazole (**3**) to produce *S*-nitroso-*N*-acetylpenicillamine (SNAP) may signify the possible formation pathway of *S*-nitrosothiols from DNICs by means of transnitrosation of *N*-nitrosamines.

Results and Discussion

Synthesis of [PPN][$(NO)_2Fe(C_{12}H_8N)_2$] ($C_{12}H_8N$ = carbazolate) (1): Addition of potassium carbazolate [K][$C_{12}H_8N$] (2 equiv) into a solution of complex [PPN][$(NO)_2Fe(SC_7H_4SN)_2$] in THF at ambient temperature led to the IR ν_{NO} stretching frequency shift from 1767 (s), 1717 (s) to 1748 (s), 1691 cm^{-1} (s), which is consistent with the ligand displacement of two $[SC_7H_4SN]^-$ groups to yield $\{Fe(NO)_2\}^9$ [PPN][$(NO)_2Fe(C_{12}H_8N)_2$] (**1**).[21] Complex **1** was characterized by IR, UV/Vis, EPR spectroscopy, and single-crystal X-ray diffraction.[22] In the isotopic labeling experiments, ^{15}NO-labeled complex **1** displays a seven-line EPR signal at $g=$ 2.023 (298 K) with the hyperfine coupling constants $a_{N(NO)}=$ 3 G and $a_{N(carbazolate)}=3.8$ G, and a rhombic EPR signal with $g_1=2.029$, $g_2=2.018$, and $g_3=2.011$ (77 K; Figure 1).[21]

Conversion of complex 1 into *N*-nitrosocarbazole (3) and *S*-nitroso-*N*-acetylpenicillamine (SNAP): Treatment of complex **1** with bis(dimethylthiocarbamoyl) disulfide ($(S_2CNMe_2)_2$; 1 equiv) led to the formation of the known $\{Fe(NO)\}^7$ [$(NO)Fe(S_2CNMe_2)_2$] (**2**) accompanied by the liberation of [PPN][$C_{12}H_8N$] characterized by ^1H NMR spectroscopy and *N*-nitrosocarbazole (**3**) (Scheme 1a and b). The shift of the IR ν_{NO} stretching frequencies from (1748, 1691) to 1715 cm^{-1} (THF) corroborated the formation of complex **2** (Figure S1 in the Supporting Information).[23] Compound **3**, isolated from reaction of complex **1** and $(S_2CNMe_2)_2$, was characterized by IR, UV/Vis, $^1H/^{15}N$ NMR spectroscopy, and single-crystal X-ray diffraction (Figure S2 in the Supporting Information). The reaction sequences given in Scheme 1, supported by the absence of released $NO_{(g)}$, may reasonably account for the transformation of complex **1** into compound **3**. Consistent with the reaction of $[(NO)_2FeS_5]^-$ and $(-SC_7H_4SN)_2$ to result in the formation of $[(NO)_2Fe(SC_7H_4SN)_2]^-$ by means of oxidative addition and the concomitant reductive elimination,[19] oxidative addition of $(S_2CNMe_2)_2$ to the $\{Fe(NO)_2\}^9$ complex **1** generated the proposed six-coordinate intermediate **A** (Scheme 1a). The subsequent chelation of $[S_2CNMe_2]^-$ ligands to Fe triggered one carbazolate to trap the nitrosyl ligand (NO^+) to yield com-

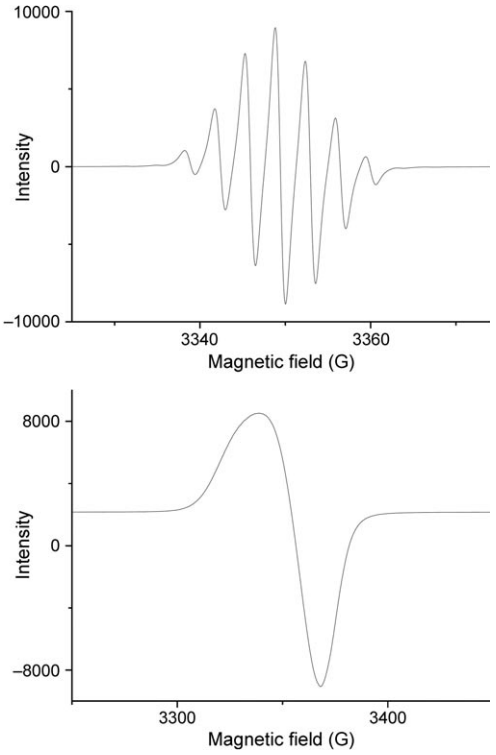

Figure 1. EPR spectra of complex **1**: a) at 298 K ($g=2.023$; $a_{N(NO)}=3$ G and $a_{N(carbazolate)}=3.8$ G), b) at 77 K ($g_1=2.029$, $g_2=2.018$, and $g_3=2.011$).

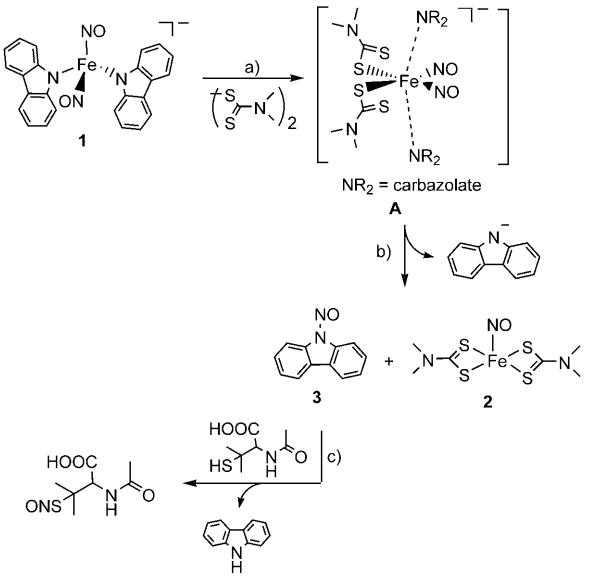

Scheme 1.

pound **3**, and the concurrent dissociation of one [PPN]-$[C_{12}H_8N]$ to lead to the formation of complex **2** (Scheme 1b). Clearly, the chelation of $[S_2CNMe_2]^-$ plays the critical role in inducing the $\{Fe(NO)_2\}^7$ intermediate **A** to convert into the $\{Fe(NO)\}^7$ complex **2** and the released compound **3**.

The S-nitrosation ability of compound **3** was displayed by reaction of **3** and *N*-acetylpenicillamine (NAP) (Scheme 1c). Similar to S-nitrosation by the aromatic and aliphatic *N*-nitrosamines,[10b,c] the appearance of an ^{15}N NMR spectroscopic signal ($\delta=447$ ppm) accompanied by the simultaneous disappearance of an ^{15}N NMR spectroscopic signal at $\delta=170$ ppm (*N*-nitrosocarbazole) indicated the formation of *S*-nitroso-*N*-acetylpenicillamine (SNAP) after the solution mixture of compound **3** and NAP (1:1 molar ratio) was stirred in $[D_6]$DMSO for 8 h (Figure S3 in the Supporting Information). This result demonstrates that DNIC **1** can be converted into *S*-nitrosothiol SNAP by means of the transnitrosation of *N*-nitrosamine **3** (Scheme 1).

$NO_{(g)}$ and nitroxyl (HNO/NO^-) derived from the reaction of complex 1 with $(PyPepS)_2$ and $[P(SX)_3]$ (X = H or Na), respectively: To elucidate the NO-releasing ability of complex **1**, the reaction of **1** and $(PyPepS)_2$ ($PyPepS=[SC_6H_4$-*o*-$NHC(O)(C_5H_4N)]_2$) was conducted. The conversion of complex **1** into complex [PPN][$Fe(PyPepS)_2$] (**4**) accompanied by the by-product carbazole upon reaction of $(PyPepS)_2$ (1 equiv) and **1** was monitored by IR ν_{NO} and ν_{CO} spectra, the disappearance of IR ν_{NO} stretching frequencies (1748 (s), 1691 cm^{-1} (s); complex **1**), and the shift of IR ν_{CO} stretching frequencies from 1691 cm^{-1} (s) ($(PyPepS)_2$) to 1677 cm^{-1} (s) (**4**) (Scheme 2). The formation of complex **4**

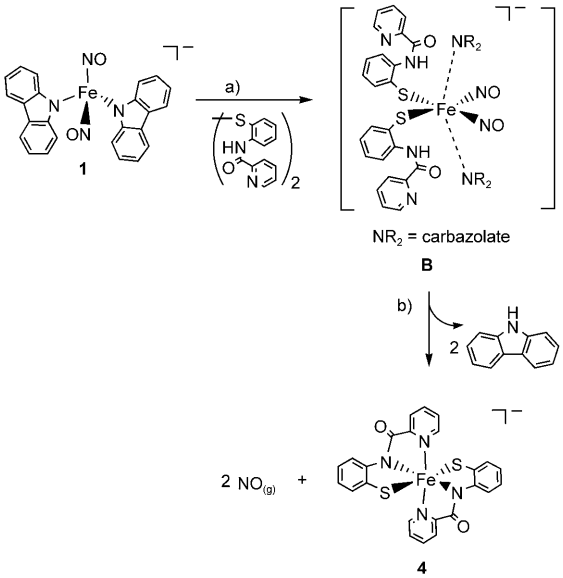

Scheme 2.

was also characterized by single-crystal X-ray diffraction (Figure S4 in the Supporting Information), and the by-product carbazole was identified by ^1H NMR spectroscopy. The released nitric oxide in the reaction of complex **1** and $(PyPepS)_2$ was trapped by complex $[S_5Fe(\mu\text{-}S)_2FeS_5]^{2-}$ to produce the known $[S_5Fe(NO)_2]^-$.[24] The transformation of complex **1** into complex **4**, carbazole, and $NO_{(g)}$ under the reaction of $(PyPepS)_2$ and **1** may be accounted for by the following reaction sequences: $(PyPepS)_2$ was oxidatively added to **1**, thus leading to the formation of intermediate **B**

(Scheme 2). As shown in Scheme 2b, it is presumed that intermediate **B** prefers the intramolecular deprotonation of the proximal carboxamide-coordinated ligands by carbazolate followed by chelation of carboxamido and pyridine to result in the formation of carbazole and **4** along with the release of $NO_{(g)}$ as opposed to the elimination of *N*-nitrosocarbazole **3** observed in the reaction of **1** and $(S_2CNMe_2)_2$. These results illustrate one aspect of how the incoming substitution ligands ($(S_2CNMe_2)_2$ versus $(PyPepS)_2$) in cooperation with the carbazolate-coordinated ligands of DNIC **1** function to control the release of NO^+ or 'NO from DNIC **1** upon reaction of **1** and the substitution ligands.

The multiple functions of DNIC **1** to serve as the [NO^+] and ['NO] donor species modulated by the distinct incoming substitution ligands provide the opportunity (methodology) to directly probe the potential of DNIC **1** to act as a nitroxyl donor species. Upon addition of $P(C_6H_3\text{-}3\text{-}SiMe_3\text{-}2\text{-}SH)_3$ ($[P(SH)_3]$) into the solution of complex **1** in THF in a 1:1 stoichiometry at 0°C, a reaction ensued over the course of 30 min to yield $[PPN][Fe(NO)P(C_6H_3\text{-}3\text{-}SiMe_3\text{-}2\text{-}S)_3]$ (**5**) and N_2O characterized by IR and single-crystal X-ray diffraction (Scheme 3a–c, Figure 2). The conversion of complex **1** into

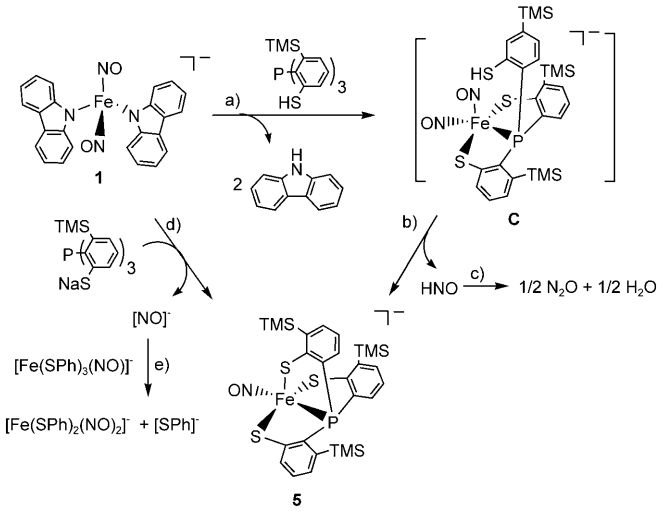

Scheme 3.

complex **5** accompanied by the formation of N_2O as byproduct under the reaction of $[P(SH)_3]$ (1 equiv) and complex **1** was monitored by IR spectroscopy; the formation of one stretching band at 2223 cm^{-1} is in accordance with the formation of N_2O, and the shift of the ν_{NO} stretching frequencies from (1748 (s), 1691 (s)) to 1720 cm^{-1} through the appearance of IR ν_{NO} (1682 (s), 1638 cm^{-1} (s)) confirms the formation of complex **5** by means of the proposed intermediate $[PPN][Fe(NO)_2P(C_6H_3\text{-}3\text{-}SiMe_3\text{-}2\text{-}S)_2(C_6H_3\text{-}3\text{-}SiMe_3\text{-}2\text{-}SH)]$ (**C**) (Scheme 3a–c).[25] The transformation of complex **1** into complex **5** along with N_2O under the reaction of $[P(SH)_3]$ and **1** may be rationalized by the following reaction sequences: protonation of the more accessible, electron-rich coordinated carbazolate by $[P(SH)_3]$ and the subsequent chelation of the phosphine and thiolate atoms to

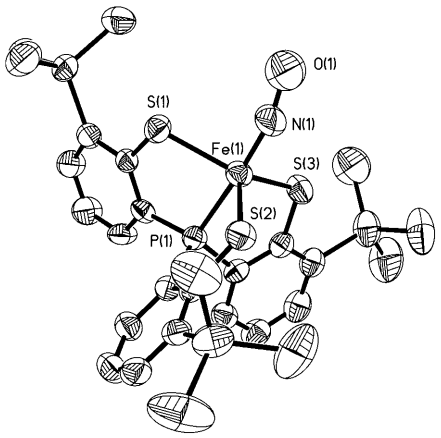

Figure 2. ORTEP drawing and labeling scheme of a complex **5** unit in $[PPN]^+$ salt with thermal ellipsoids drawn at 50% probability. Disorder of O(1) and O(1′) atoms of complex **5** was observed with equal occupancy factors of 50%. Selected bond lengths [Å] and angles [°]: Fe–N(1) 1.632(4), Fe–P(1) 2.210(1), Fe–S(1) 2.325(1), Fe–S(2) 2.285(1), Fe–S(3) 2.281(1), O(1)–N(1) 1.259(9), O(1′)–N(1) 1.153(9); N(1)-Fe-P(1) 174.48(17), N(1)-Fe-S(1) 93.95(15), N(1)-Fe-S(2) 101.15(18), N(1)-Fe-S(3) 95.85(15), P(1)-Fe-S(1) 81.72(4), P(1)-Fe-S(2) 83.83(4), P(1)-Fe-S(3) 84.04(4), S(2)-Fe-S(1) 114.43(5), S(2)-Fe-S(3) 115.34(5), S(1)-Fe-S(3) 126.02(5), O(1)-N(1)-Fe 152.5 (6), O(1′)-N(1)-Fe 162.8 (7).

iron led to the formation of intermediate **C** (Scheme 3a).[25] The adjacent NO-coordinated ligand of the $\{Fe(NO)_2\}^9$ intermediate **C** is partially polarized on the approach of the *exo*-thiol proton to promote the "induced internal electron transfer" from Fe to the redox-noninnocent NO-coordinated ligand. The higher-electron-density NO ligand of intermediate **C** may act as $[NO]^-$ (nitroxyl) to facilitate deprotonation of the intramolecular thiol, thus leading to the formation of **5** and HNO (Scheme 3b).[25] The subsequent dimerization of HNO followed by dehydration rationalized the formation of N_2O (Scheme 3c).

To further corroborate the generation of HNO as byproduct in the above reaction and to demonstrate the potential of DNIC **1** to act as a nitroxyl-releasing species regulated by the substitution ligands, the reactivity of complex **1** toward $P(C_6H_3\text{-}3\text{-}SiMe_3\text{-}2\text{-}SNa)_3$ ($[P(SNa)_3]$) was investigated. The shift of the IR ν_{NO} stretching frequencies from (1748, 1691) to 1720 cm^{-1} (THF) corroborated the formation of complex **5** upon addition of $[P(SNa)_3]$ (1 equiv) into the solution of **1** in THF at 0°C. The subsequent addition of a solution of $[PPN][(^{15}NO)Fe(SPh)_3]$ in THF into the mixture solution of complex **1** and $[P(SNa)_3]$ to yield $[PPN][(^{15}NO)(^{14}NO)Fe(SPh)_2]$ (1732 (sh), 1693 (s), 1670 cm^{-1} (s)) and $[SPh]^-$ rationalized the generation of nitroxyl anion in the reaction of complex **1** and $[P(SNa)_3]$ (Scheme 3d and e), in contrast to nitrosylation of complex $[(NO)Fe(SPh)_3]^-$ to yield $[PPN][(NO)_2Fe(SPh)_2]$ along with $(PhS)_2$ and the reaction of $[(NO)Fe(SPh)_3]^-$ with $[NO][BF_4]$ to lead to $[(NO)_2Fe(\mu\text{-}SPh)_2Fe(NO)_2]$ accompanied by $(PhS)_2$.[26] The formation of **5** as well as the absence of NO radical and N_2O (IR 2223 cm^{-1}) supported the generation of nitroxyl anion in the reaction of complex **1** and $[P(SNa)_3]$. Thus, the

presence of chelating ligand $[P(SNa)_3]$ appears to be crucial in triggering DNIC **1** to act as a nitroxyl-donor species and the conversion of DNIC **1** into complex **5**.

Structure: The structure of complex **1** in the sodium crown ether salt $[Na([18]crown-6)]^+$, derived from reaction of complex $[Na([18]crown-6)][(NO)_2Fe(SC_7H_4SN)_2]$ and potassium carbazolate $[K][C_{12}H_8N]$ (2 equiv), is shown in Figure 3. The

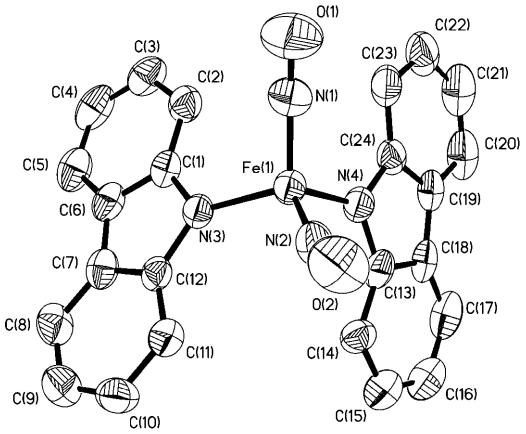

Figure 3. ORTEP drawing and labeling scheme of a complex **1** unit in $[Na([18]crown-6)]^+$ salt with thermal ellipsoids drawn at 50% probability. Selected bond lengths [Å] and angles [°]: Fe–N(1) 1.663(6), Fe–N(2) 1.683(6), Fe–N(3) 1.952(4), Fe–N(4) 1.973(5), O(1)–N(1) 1.182(7), O(2)–N(2) 1.164(7); N(1)-Fe-N(2) 109.4(3), N(1)-Fe-N(3) 109.9(2), N(2)-Fe-N(3) 114.5(2), N(1)-Fe-N(4) 111.4(3), N(2)-Fe-N(4) 107.3(2), N(3)-Fe-N(4) 104.2(2), O(1)-N(1)-Fe 165.5 (6), O(2)-N(2)-Fe 160.0 (5).

Fe–N(3) and Fe–N(4) bond lengths of 1.952(4) and 1.973(5) Å observed in complex **1** are comparable with the reported $Fe–N_{(Im)}$ bond lengths of 1.978(3) and 1.974(3) Å obtained in $[(NO)_2Fe(C_3H_3N_2)_2]^-$.[21] The average $Fe–N_{(NO)}$ bond length of 1.673(6) Å, which falls in the range 1.661(4)–1.695(3) Å, and the average N–O bond length of 1.173(7) Å, which falls in the range 1.160(6)–1.178(3) Å, are consistent with those of the anionic $\{Fe(NO)_2\}^9$ DNICs.[21c]

Figure 2 displays the thermal ellipsoid plot of the anionic complex **5** and selected bond lengths and angles are given in the figure captions. The N(1)-Fe-P(1), S(2)-Fe-S(1), S(2)-Fe-S(3), and S(1)-Fe-S(3) bond angles of 174.48(17), 114.43(5), 115.34(5), and 126.02(5)°, respectively, are consistent with the nearly regular trigonal bipyramidal coordination environment about Fe of complex **5**. In contrast to the linear Fe-N-O bond of the $\{Fe(NO)\}^6$ complex $[Fe(NO)(PS'_3)]$ ($PS'_3 = P(C_6H_3\text{-}3\text{-}Ph\text{-}2\text{-}SH)_3$) (bond angle 175.2(3)°; Table 1),[27a] the bent Fe-N-O bond with a bond angle of 152.5(6)/162.8(7)° for $\{Fe(NO)\}^7$ complex **5** suggests the presence of an $\{Fe^{II}(^{\bullet}NO)\}^7$ electronic structure.[27b] Also, the electronic effect from $\{Fe(NO)\}^6$ $[Fe(NO)(PS'_3)]$ to $\{Fe(NO)\}^7$ complex **5** may rationalize the observed lengthening of the N–O bond length (1.154(5) Å for $\{Fe(NO)\}^6$ $[Fe(NO)(PS'_3)]$ vs. 1.259(9) Å for $\{Fe(NO)\}^7$ complex **5**) and the shortening of the Fe–N(O) bond length (1.676(3) Å for $\{Fe(NO)\}^6$ $[Fe(NO)(PS'_3)]$ vs. 1.632(4) Å for $\{Fe(NO)\}^7$ complex **5**).

Table 1. Selected bond lengths [Å] and angles [°] for complex **5** and $[Fe(NO)(PS'_3)]$.[27a]

	5	$[Fe(NO)(PS'_3)]$
Fe–S[a]	2.297(1)	2.244(1)
Fe–N	1.632(4)	1.676(3)
N–O	1.259(9)	1.154(5)
	1.153(9)	
Fe–P(N)	2.210(1)	2.240(1)
∢Fe-N-O	152.5(6)	175.2(3)
	162.8(7)	–
geometry	trigonal bipyramidal	trigonal bipyramidal

[a] Average bond length.

Conclusion

Studies on the transformation of DNIC **1** into *N*-nitrosocarbazole ($R_2N–NO$) and then *S*-nitroso-*N*-acetylpenicillamine (RSNO), and on the production of $NO_{(g)}$ and nitroxyl (HNO/NO^-) derived from DNIC **1**, respectively, led to the following results.

As shown in Scheme 4, reaction of DNIC **1** and the incoming ligands $(S_2CNMe_2)_2$, $(PyPepS)_2$, and $P(C_6H_3\text{-}3\text{-}SiMe_3\text{-}2\text{-}SH)_3$) yielded complex **2**, complex **4**, and complex **5**

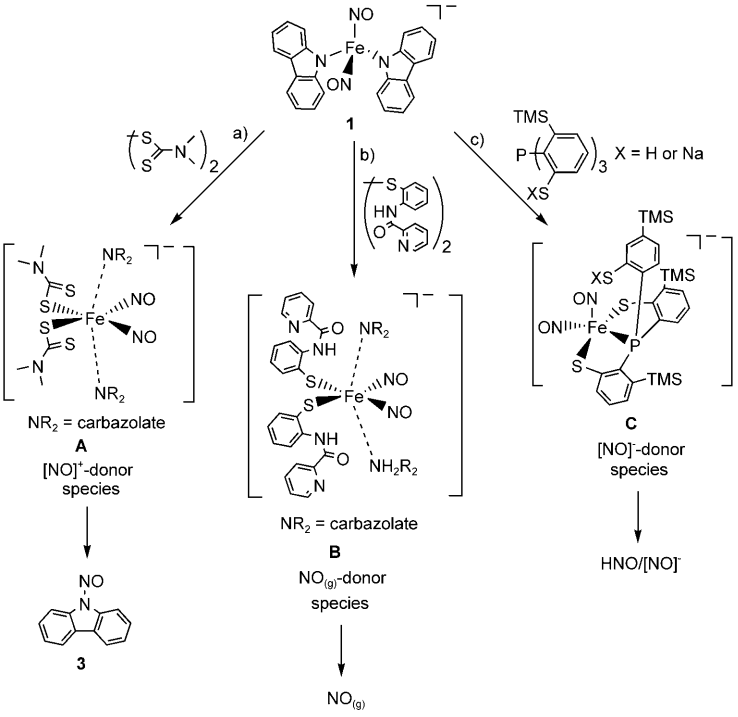

Scheme 4.

through intermediates **A**, **B**, and **C**, respectively. The incoming substitution ligands play a key role in tuning the geometric structure and the electronic structure of the intermediates and the final products to conduct the release of $[NO]^+$, $^{\bullet}NO$, and $[NO]^-$, respectively.

In contrast to the transformation of $[(NO)_2FeS_5]^-$ into $[(NO)_2Fe(SC_7H_4SN)_2]^-$ facilitated by $(-SC_7H_4SN)_2$,[19] the incoming substitution ligand ($(S_2CNMe_2)_2$) plays a critical role

in triggering the buildup of the proposed anionic $\{Fe(NO)_2\}^7$ $[(NO)_2Fe(S_2CNMe_2)_2(NR_2)_2]^-$ (NR_2 = carbazolate) (**A**) intermediate, and subsequently, serves to induce intramolecular NO^+ transfer to produce *N*-nitrosocarbazole in the reaction of DNIC **1** and $(S_2CNMe_2)_2$ (Scheme 4a). Intramolecular N-nitrosation of the carbazolate elicited from DNIC **1** and the subsequent NO^+ transfer from *N*-nitrosocarbazole to *N*-acetylpenicillamine to yield SNAP demonstrates that the interconversion between DNICs and *N*-nitrosamines (R_2N–NO)/*S*-nitrosothiols (RSNO) is reversible.[28]

As shown in Scheme 4b, the reaction of DNIC **1** and $(PyPepS)_2$ produced the proposed anionic $\{Fe(NO)_2\}^7$ $[(NO)_2Fe(PyPepS)_2(NR_2)_2]^-$ (NR_2 = carbazolate) intermediate (**B**). The intramolecular deprotonation of the adjacent carboxyamide by carbazolate and the subsequent chelation of $[PyPepS]^{2-}$ trigger the release of the ˙NO radical.

Compared to the buildup of the proposed anionic $\{Fe(NO)_2\}^7$ intermediates in the reaction of DNIC **1** and $(S_2CNMe_2)_2$/$(PyPepS)_2$ disulfides, respectively, formation of the anionic $\{Fe(NO)_2\}^9$ intermediate **C** induced the release of HNO by means of the nitroxyl-facilitating intramolecular thiol deprotonation in the reaction of DNIC **1** and $P(C_6H_3$-3-$SiMe_3$-2-$SH)_3$) (Scheme 4c). Alternatively, the nucleophilic attack of the chelating $[P(SNa)_3]$ on DNIC **1** triggered the direct release of $[NO]^-$.

Clearly, the highly reactive intermediates **A**, **B**, and **C** optimize the electronic and structural property of the $\{Fe(NO)_2\}$ core for its required $[NO]^+$, [˙NO], and $[NO]^-$ donor function. DNIC **1** acting as $[NO]^+$, [˙NO], and $[NO]^-$ donor species may also support the assignment of the resonance hybrids of $\{Fe^{III}(NO^-)_2\}^9$, $\{Fe^{I}(^{\bullet}NO)_2\}^9$ and $\{Fe^{1-}(NO^+)_2\}^9$ electronic structures of DNICs reported in the previous study.[19,20]

N-Nitrosation of tryptophan is well documented (e.g., the reported concurrent presence of *S*-nitrosocysteine and *N*-nitrosotryptophan of serum albumin identified in human plasma).[29] On the basis of the inhibition of glutathione reductase by means of nitrosation of His467 reported by Mülsch et al., N-nitrosation is regarded as another mechanism by which proteins are post-translationally modified in the NO-mediated signal transduction.[3] This study signifies that DNICs attached to the tryptophan residue, derived from a ligand-exchange reaction or nitrosylation of Rieske-type [Fe–S] proteins, may trigger the direct N-nitrosation of the intramolecular tryptophan by means of a reaction with the oxidized cysteine in a biological system.[21] Specifically, in cooperation with the NO transfer from *N*-nitrosamines to thiols, DNICs may act as the endogenous NO carrier to nitrosate the thiol side chain of cysteine by means of transnitrosation of *N*-nitrosotryptophan. The intramolecular N-nitrosation of the coordinated carbazolate of DNIC **1** observed in this study may lend support to the direct S-nitrosation of the intramolecular $[SR]^-$ ligand of DNICs that leads to the formation of *S*-nitrosothiols. Of importance, in addition to the oxidation state of the intrinsic NO ligand of DNICs modulated by the coordinated ligands,[19,20] the unique DNIC is also capable of generating the distinct redox-interrelated forms of NO regulated by the incoming substitution ligands. This result may also signify that the generation of the various forms of NO from DNICs may be regulated by the oxidation state of the incoming Cys ligand and the protein structure in the immediate vicinity in biological systems. Presumably, DNICs may act as an intermediary of NO in the redox signaling processes by providing the distinct redox-interrelated forms of NO to interact with different NO-responsive targets in biological systems. Also, in combination with measuring the conversion of DNIC into R_2N–NO or $NO_{(g)}$ released from DNIC, the existence of DNICs in biological systems could be quantified through the chemiluminescence method. This study not only signifies the NO signaling processes initiated by DNICs in biological systems but also develops a promising avenue for DNICs in medicinal chemistry.

Experimental Section

General: Manipulations, reactions, and transfers were conducted under nitrogen according to Schlenk techniques or in a glove box (argon gas). Solvents were distilled under nitrogen from appropriate drying agents (diethyl ether from CaH_2; acetonitrile from CaH_2/P_2O_5; methylene chloride from CaH_2; hexane and tetrahydrofuran (THF) from sodium benzophenone) and stored in dried, N_2-filled flasks over 4 Å molecular sieves. Nitrogen was purged through these solvents before use. The solvent was transferred to the reaction vessel through stainless cannula under positive pressure of N_2. The reagents potassium carbazolate (TCI), bis(dimethylthiocarbamoyl) disulfide (Aldrich), and *N*-acetylpenicillamine (Fluka) were used as received. Compounds $[SC_6H_4$-*o*-$NHC(O)(C_5H_4N)]_2$ ($(PyPepS)_2$), $P(C_6H_3$-3-$SiMe_3$-2-$SH)_3$ ($P(SH)_3$), and $[PPN][(NO)_2Fe(SC_7H_4SN)_2]$ were synthesized by published procedures.[19,30] ^{15}N-labeled complex $[PPN][(^{15}NO)_2Fe(SC_7H_4SN)_2]$ and $[PPN][(NO)Fe(SPh)_3]$ were synthesized on the basis of published procedures by using $[PPN][^{15}NO_2]$.[19,20,26] Compound $P(C_6H_3$-3-$SiMe_3$-2-$SNa)_3$ was obtained by reaction of $P(C_6H_3$-3-$SiMe_3$-2-$SH)_3$ and NaOMe in MeOH. Infrared spectra of the ν_{NO} stretching frequencies were recorded using a Perkin–Elmer model spectrum One B spectrometer with sealed solution cells (0.1 mm, CaF_2 windows). UV/Vis spectra were recorded using a Jasco V-570 spectrometer. ^1H and ^{15}N NMR spectra were obtained using a Varian Unity-500 spectrometer. Chemical shifts (δ) of ^{15}N NMR spectra are relative to neat nitromethane ($\delta = 0$ ppm) as the external standard. Analyses of carbon, hydrogen, and nitrogen were obtained using a CHN analyzer (Heraeus).

Preparation of [cation][$(NO)_2Fe(C_{12}H_8N)_2$] ($C_{12}H_8N$ = carbazolate; cation = bis(triphenylphospine)iminium (PPN^+) or [Na([18]crown-6)]$^+$) (1): Complexes $[PPN][(NO)_2Fe(SC_7H_4SN)_2]$ (0.368 g, 0.5 mmol) and potassium carbazolate ($[K][C_{12}H_8N]$) (0.205 g, 1.0 mmol) were dissolved in THF (10 mL) and stirred for 10 min under nitrogen at ambient temperature.[19] The reaction was monitored with FTIR. The IR ν_{NO} stretching frequencies shifted from 1767 (s), 1717 (s) to 1748 (s), 1691 cm^{-1} (s). The reaction solution was filtered through Celite to remove the insoluble $[PPN][SC_7H_4SN]$. Hexane was then added to the filtrate (solution in THF), thus leading to the precipitation of a purple solid, $[PPN][(NO)_2Fe(C_{12}H_8N)_2]$ (**1**) (yield 0.850 g, 86%). Complex **1** in [Na([18]crown-6)]$^+$ salt was obtained from the reaction of complex [Na([18]crown-6)] $[(NO)_2Fe(SC_7H_4SN)_2]$ and potassium carbazolate $[K][C_{12}H_8N]$ (2 equiv) in THF. Single crystals of complex **1** in [Na([18]crown-6)]$^+$ salt, suitable for single-crystal X-ray diffraction, were obtained by layering the solution of [Na([18]crown-6)]$[(NO)_2Fe(C_{12}H_8N)_2]$ in THF with diethyl ether for 2 d. IR (THF): $\tilde{\nu}$ = 1748 (s), 1691 cm^{-1} (s) (NO); UV/Vis (THF): λ_{max} (ε) = 355 (6000), 524 (700), 724 nm (300 $mol^{-1}dm^3cm^{-1}$); elemental analy-

sis calcd (%) for $C_{60}H_{46}FeN_5O_2P_2$: C 73.03, H 4.70, N 7.10; found: C 73.43, H 5.00, N 7.90. The ^{15}N-labeled complex **1** was prepared in the same manner by reaction of complex $[PPN][(^{15}NO)_2Fe(SC_7H_4SN)_2]$ and potassium carbazolate (2 equiv). IR (THF): $\tilde{\nu}=1714$ (s), 1657 cm^{-1} (s; ^{15}NO).

Reaction of bis(dimethylthiocarbamoyl) disulfide (DTC) and 1: Bis(dimethylthiocarbamoyl) disulfide (DTC; 0.048 g, 0.2 mmol) and complex **1** (0.198 g, 0.2 mmol) were dissolved in THF (5 mL) and stirred for 4 h at ambient temperature under an N_2 atmosphere. The IR ν_{NO} spectrum showed a strong absorption band at 1715 cm^{-1} (THF) assigned to the formation of the known complex $[(NO)Fe(S_2CNMe_2)_2]$ (**2**).[23] The solution in THF was filtered through Celite to remove the insoluble $[PPN][C_{12}H_8N]$ solid characterized by ^1H NMR spectroscopy ($[D_6]$DMSO): $\delta=$ 8.04 (d), 7.79 (m), 7.46 (m), 7.30 (t), 7.05 ppm (t). Addition of hexane (20 mL) to the filtrate (THF) led to the precipitation of green solid $[(NO)Fe(S_2CNMe_2)_2]$ (**2**) (yield 0.058 g, 89%). The upper-layer THF/hexane solution was transferred to the another flask through a stainless steel cannula and dried under vacuum to obtain *N*-nitrosocarbazole (**3**). Compound **3** was redissolved in hexane and kept in the refrigerator at −20 °C for 2 d. Pale-yellow crystals suitable for X-ray diffraction analysis were obtained (0.016 g, 42%). Compound **3**: ^1H NMR (500 MHz, $[D_6]$DMSO, TMS): $\delta=8.43$ (d), 8.21 (d), 8.16 (m), 7.61 (t), 7.56 ppm (m); ^{15}N NMR (500 MHz, $[D_6]$DMSO, nitromethane): $\delta=170$ ppm (s); IR (KBr): $\tilde{\nu}=1491$ cm^{-1} (s) (NO); UV/Vis (THF): λ_{max} (ε) = 281 (11200), 331 (9920), 414 (300), 434 nm (200 $mol^{-1}dm^3cm^{-1}$); elemental analysis calcd (%) for $C_{13}H_{12}N_2O$: C 73.56, H 5.70, N 13.20; found: C 73.46, H 6.36, N 13.70. The ^{15}N-labeled compound **3** was prepared in the same manner by reaction of complex $[PPN][(^{15}NO)_2Fe(C_{12}H_8N)_2]$ and DTC (1 equiv). IR (KBr): $\tilde{\nu}=1462$ cm^{-1}(s; ^{15}NO).

Reaction of compound 3 and *N*-acetylpenicillamine (NAP): $[D_6]$DMSO (1 mL) was added to a 30 mL Schlenk flask loaded with compound **3** (0.099 g, 0.5 mmol) and *N*-acetylpenicillamine (NAP; 0.096 g, 0.5 mmol). The reaction solution was stirred at ambient temperature for 8 h and monitored with ^{15}N NMR spectroscopy. The disappearance of the ^{15}N NMR chemical shift at $\delta=170$ ppm and the appearance of the chemical shift at $\delta=447$ ppm were observed. THF (1 mL) and diethyl ether (20 mL) were then added to the solution in $[D_6]$DMSO, thus leading to the precipitation of the known green solid *S*-nitroso-*N*-acetylpenicillamine (SNAP; 0.099 g, 90%).[10b,c] The solution in $[D_6]$DMSO/THF/diethyl ether was then transferred into another flask through a stainless steel cannula under positive nitrogen pressure and dried under vacuum to obtain carbazole as identified by ^1H NMR spectroscopy ($[D_6]$DMSO): $\delta=11.23$ (s), 8.09 (d), 7.48 (d), 7.37 (m), 7.15 ppm (m).

Reaction of $(PyPepS)_2$ (PyPepS=$[SC_6H_4$-*o*-$NHC(O)(C_5H_4N)]_2$) and 1: A solution of THF (5 mL) and complex **1** (0.198 g, 0.2 mmol) was prepared under an N_2 atmosphere in a vial. The vial containing the solution of **1** in THF was then placed in a larger vial containing a solution of $[PPN]_2[S_5Fe(\mu\text{-}S)_2FeS_5]$ in THF/CH_3CN (0.157 g, 0.1 mmol) and the large vial was capped with a well-sealed septum. A solution of *N*-2-mercaptophenyl-2′-pyridinecarboxamide disulfide ($(PyPepS)_2$) (0.2 mmol, 0.092 g) in THF (5 mL) was then added into the vial containing the solution of **1** in THF by using a gas-tight syringe. The mixture solution was stirred at ambient temperature for 8 h. The resulting solution kept in the larger vial was transferred to another tube and dried under vacuum. The crude solid was redissolved in THF and filtered through Celite to remove the insoluble solid. Addition of hexane to the filtrate led to the precipitation of the known complex $[PPN][S_5Fe(NO)_2]$ (0.044 g, 27%) characterized by IR spectroscopy.[24] In the meantime, hexane (20 mL) was added to the brown reaction solution kept in the small vial to result in the precipitation of the insoluble brown solid $[PPN][Fe(PyPepS)_2]$ (**4**) (0.177 g, 84%) characterized by IR ($\nu_{CO}=1677$ cm^{-1} (s) (CH_3CN)) and UV/Vis (438, 520, 880 nm (DMF)). The upper solution (THF/hexane) was dried under vacuum to obtain carbazole as characterized by ^1H NMR spectroscopy. Brown crystals suitable for X-ray diffraction analysis were isolated from the solution of DMF and complex **4** layered with diethyl ether and hexane at −20 °C for 4 d.

Reaction of $P(SH)_3$ ($P(SH)_3=P(C_6H_3$-3-$SiMe_3$-2-$SH)_3$) and 1: THF (3 mL) was added through a gas-tight syringe to a 30 mL Schlenk flask loaded with complex **1** (0.198 g, 0.2 mmol) and $P(SH)_3$ (0.115 g, 0.2 mmol) at 0 °C. The reaction solution was monitored by FTIR. The IR ν_{NO} shifted from (1748 (s), 1691 (s)) to (1682 (s), 1638 cm^{-1} (s)) when the reaction solution was stirred for 10 min. The IR ν_{NO} further shifted to 1720 cm^{-1} after the reaction solution was stirred for another 20 min at ambient temperature. The IR stretching frequency located at 2223 cm^{-1}, assigned to the formation of N_2O, was observed. Hexane was then added to lead to the precipitation of the dark green solid $[PPN][Fe(PS_3)(NO)]$ (**5**) (yield 0.210 g, 88%) characterized by IR, UV/Vis, and single-crystal X-ray diffraction. The carbazole by-product that was dissolving in the THF/hexane solution was isolated and characterized by ^1H NMR spectroscopy. Recrystallization from THF solution of complex **5** layered with hexane at −20 °C for 4 d led to the dark green crystals suitable for X-ray crystallography. Complex **5**: IR (THF): $\tilde{\nu}=1720$ cm^{-1} (NO); UV/Vis (THF): λ_{max} (ε) = 526 (1800), 579 nm (2000 $mol^{-1}dm^3cm^{-1}$); elemental analysis calcd (%) for $C_{63}H_{66}FeN_2OP_3S_3Si_3$: C 63.24, H 5.56, N 2.34; found: C 63.02, H 4.98, N 2.77.

Reaction of $P(SNa)_3$ ($P(SNa)_3=P(C_6H_3$-3-$SiMe_3$-2-$SNa)_3$) and complex 1: Compounds $P(SNa)_3$ (0.128 g, 0.2 mmol) and **1** (0.198 g, 0.2 mmol) were dissolved in THF (3 mL) and stirred under N_2 at 0 °C for 5 min. The reaction was monitored with FTIR, and the IR ν_{NO} shifting from (1748 (s), 1691 (s)) to 1720 cm^{-1} (s) implied the formation of complex **5**. A solution of THF (3 mL) and $[PPN][(^{15}NO)Fe(SPh)_3]$ was immediately added to the mixture solution and monitored with FTIR. The appearance of IR ν_{NO} stretching frequencies at 1732 (sh), 1693 (s), and 1670 cm^{-1} (s) was assigned to the formation of $[PPN][(^{15}NO)(^{14}NO)Fe(SPh)_2]$,[26] comparable to the authentic complex $[PPN][(^{15}NO)(^{14}NO)Fe(SPh)_2]$ prepared by reaction of $[PPN][(^{15}NO)Fe(SPh)_3]$ and $^{14}NO_{(g)}$ (1 equiv). The mixture solution was filtered through Celite to remove the insoluble $[PPN][C_{12}H_8N]$ solid characterized by ^1H NMR spectroscopy. The addition of diethyl ether (6 mL) to the solution in THF led to the precipitation of the insoluble [PPN][SPh] solid characterized by ^1H NMR spectroscopy. More diethyl ether (6 mL) was added to the solution in THF/diethyl ether to separate the insoluble complex **5** (0.016 g, 67%), characterized by IR and UV/Vis, and the upper solution. The upper solution was then dried under vacuum to yield the brown solid $[PPN][(^{15}NO)(^{14}NO)Fe(SPh)_2]$ (0.007 g, 42%) characterized by IR and UV/Vis spectroscopy.[26]

EPR measurements: X-band EPR measurements were performed using a Bruker EMX spectrometer equipped with a Bruker TE102 cavity. The microwave frequency was measured with a Hewlett–Packard 5246L electronic counter. X-band EPR spectra of complex **1** frozen in THF were obtained with a microwave power of 19.971 mW, frequency at 9.483 GHz, and modulation amplitude of 0.1 G at 100 KHz.

Crystallography: The crystals of complexes **1**, **3**, **4**, and **5** chosen for X-ray diffraction studies measured 0.28×0.18×0.07, 0.56×0.30×0.11, 0.45×0.36×0.24, and 0.29×0.23×0.12 mm in size, respectively. Each crystal was mounted on a glass fiber and quickly coated in epoxy resin. Unit-cell parameters were obtained by least-squares refinement. Diffraction measurements for complexes **1**, **3**, **4**, and **5** were carried out using a SMART Apex CCD diffractometer with graphite-monochromated $Mo_{K\alpha}$ radiation ($\lambda=0.7107$ Å) and between 2.03 and 25.02° for complex **1**, between 1.20 and 25.03° for complex **3**, between 1.69 and 25.03° for complex **4**, and between 2.18 and 24.98° for complex **5**. Disorder of N(4)/N(4′) atoms and O(2)/O(2′) atoms of compound **3** was observed with equal occupancy factors of 50%. Disorder of O(1) and O(1′) atoms of complex **5** was observed with equal occupancy factors of 50%. Least-squares refinement of the positional and anisotropic thermal parameters of all non-hydrogen atoms and fixed hydrogen atoms were based on F^2. A SADABS[31] absorption correction was made. The SHELXTL[32] structure refinement program was employed.

Acknowledgements

We gratefully acknowledge financial support from the National Science Council of Taiwan. The authors would also like to thank Pei-Lin Chen and Ting-Shen Kuo for the single-crystal X-ray structural determinations.

[1] a) J. S. Stamler, D. J. Singel, J. Loscalzo, *Science* **1992**, *258*, 1898–1902; b) J. S. Stamler, *Cell* **1994**, *78*, 931–936.

[2] a) Y.-M. Kim, H.-T. Chung, R.-L. Simmons, T.-R. Billiars, *J. Biol. Chem.* **2000**, *275*, 10954–10961; b) F. Terenzi, M. J. Diaz-Guerra, M. Casado, S. Hortelano, S. Leoni, L. Bosca, *J. Biol. Chem.* **1995**, *270*, 6017–6021; c) Y. M. Kim, M. E. de Vera, S. C. Watkins, T.-R. Billiars, *J. Biol. Chem.* **1997**, *272*, 1402–1411; d) Y. M. Kim, R. V. Talanian, T.-R. Billiars, *J. Biol. Chem.* **1997**, *272*, 31138–31148; e) S. Dimmeler, J. Haendeler, M. Nehls, A. M. Zeiher, *J. Exp. Med.* **1997**, *185* 601–608.

[3] M. Boese, M. A. Keese, K. Becker, R. Busse, A. Mülsch, *J. Biol. Chem.* **1997**, *272*, 21767–21773.

[4] a) B. Mayer, A. L. Kleschyov, H. Stessel, M. Russwurm, T. Münzel, D. Koesling, K. Schmidt, *Mol. Pharm.* **2009**, *75*, 886–891; b) A. Friebe, D. Koesling, *Circ. Res.* **2003**, *93*, 96–105.

[5] a) J. C. Toledo, C. A. Bosworth, Jr., S. W. Hennon, H. K. Mahtani, H. A. Bergonia, J. R. Lancaster, Jr., *J. Biol. Chem.* **2008**, *283*, 28926–28933; b) H. Lewandowska, S. Meczynska, B. Sochanowicz, J. Sadlo, M. Kruszewski, *J. Biol. Inorg. Chem.* **2007**, *12*, 345–352; c) R. N. Watts, C. Hawkins, P. Ponka, D. R. Richardson, *Proc. Natl. Acad. Sci. USA* **2006**, *103*, 7670–7675; d) D. R. Richardson, H. C. Lok, *Biochim. Biophys. Acta* **2008**, *1780*, 638–651.

[6] a) S. T. Pullan, M. D. Gidley, R. A. Jones, J. Barret, T. M. Stevanin, R. C. Read, J. Freen, R. K. Poole, *J. Bacteriol.* **2007**, *189*, 1845–1855; b) A. Singh, L. Guidry, K. V. Narasimhulu, D. Mai, J. Trombley, K. E. Redding, G. I. Giles, J. R. Lancaster, A. J. C. Steyn, *Proc. Natl. Acad. Sci. USA* **2007**, *104*, 11562–11567.

[7] a) M. P. Doyle, S. N. Mahapatro, R. D. Broene, J. K. Guy, *J. Am. Chem. Soc.* **1988**, *110*, 593–599; b) T. Turk, T. C. Hollocher, *Biochem. Biophys. Res. Commun.* **1992**, *183*, 983–988; c) M. E. Murphy, H. Sies, *Proc. Natl. Acad. Sci. USA* **1991**, *88*, 10860–10864; d) J. M. Fukuto, G. C. Wallace, R. Hszieh, G. Chaudhuri, *Biochem. Pharmacol.* **1992**, *43*, 607–613; e) K. M. Miranda, *Coord. Chem. Rev.* **2005**, *249*, 433–455; f) J. M. Fukuto, C. H. Switzer, K. M. Miranda, D. A. Wink, *Annu. Rev. Pharmacol. Toxicol.* **2005**, *45*, 335–355.

[8] D. T. Hess, A. Matusmoto, S.-O. Kim, H. E. Marshall, J. S. Stamler, *Nat. Rev. Mol. Cell Biol.* **2005**, *6*, 150–166.

[9] a) N. S. Bryan, T. Rassaf, R. E. Maloney, C. M. Rodriguez, F. Saiji, J. R. Rodriguez, M. Feelisch, *Proc. Natl. Acad. Sci. USA* **2004**, *101*, 4308–4313; b) M. G. Espey, K. M. Miranda, D. D. Thomas, D. A. Wink, *J. Biol. Chem.* **2001**, *276*, 30085–30091; c) M. A. Moro, V. M. Darley-Usmar, D. A. Goodwin, N. G. Read, R. Zamora-Pino, M. Feelisch, M. W. Radomski, S. Moncada, *Proc. Natl. Acad. Sci. USA* **1994**, *91*, 6702–6706.

[10] a) J. S. Scharfstein, J. F. Keany, A. Slivka, G. N. Welch, J. A. Vita, J. S. Stamler, J. Loscalzo, *J. Clin. Invest.* **1994**, *94*, 1432–1439; b) K. Sonnenschein, H. de Groot, M. Kirsch, *J. Biol. Chem.* **2004**, *279*, 45433–45440; c) T. Yanagimoto, T. Toyota, N. Matsuki, Y. Makino, S. Uchiyama, T. Ohwada, *J. Am. Chem. Soc.* **2007**, *129*, 736–737; d) A. Weichsel, E. M. Maes, J. F. Anderson, J. G. Valenzuela, T. K. Shokhireva, F. A. Walker, W. R. Montfort, *Proc. Natl. Acad. Sci. USA* **2005**, *102*, 594–599; e) B. P. Luchsinger, E. N. Rich, A. J. Gow, E. M. Williams, J. S. Stamler, D. J. Singel, *Proc. Natl. Acad. Sci. USA* **2003**, *100*, 461–466.

[11] a) J. R. Lancaster Jr. , J. B. Hibbs, Jr., *Proc. Natl. Acad. Sci. USA* **1990**, *87*, 1223–1227; b) M. W. Foster, J. A. Cowan, *J. Am. Chem. Soc.* **1999**, *121*, 4093–4100; c) C. E. Cooper, *Biochim. Biophys. Acta Bioenerg.* **1999**, *1411*, 290–309; d) A. R. Butler, I. L. Megson, *Chem. Rev.* **2002**, *102*, 1155–1166; e) T. Ueno, Y. Susuki, S. Fujii, A. F. Vanin, T. Yoshimura, *Biochem. Pharmacol.* **2002**, 63, 485–493; f) J. A. McCleverty, *Chem. Rev.* **2004**, *104*, 403–418.

[12] a) C. A. Bosworth, J. C. Toledo, Jr., J. W. Zmijewski, Q. Li, J. R. Lancaster, Jr., *Proc. Natl. Acad. Sci.* **2009**, *106*, 4671–4676; b) M. Boese, P. I. Mordvintcev, A. F. Vanin, R. Busse, A. Mülsch, *J. Biol. Chem.* **1995**, *270*, 20244–29249.

[13] J. H. Enemark, R. D. Feltham, *Coord. Chem. Rev.* **1974**, *13*, 339–406.

[14] L. L. Perissinotti, D. A. Estrin, G. Leitus, F. Doctorovich, *J. Am. Chem. Soc.* **2006**, *128*, 2512–2513.

[15] J. Lee, G. B. Richter-Addo, *J. Inorg. Biochem.* **2004**, *98*, 1247–1250.

[16] K. B. Capps, A. Bauer, K. Sukcharoenphon, C. D. Hoff, *Inorg. Chem.* **1999**, *38*, 6206–6211.

[17] a) Y. Liu, M. D. Ryan, *J. Electroanal. Chem.* **1994**, *368*, 209–219; b) D. Lancon, K. M. Kadish, *J. Am. Chem. Soc.* **1983**, *105*, 5610–5617; c) I. K. Choi, Y. Liu, D. Feng, K. J. Paeng, M. D. Ryan, *Inorg. Chem.* **1991**, *30*, 1832–1839; d) J. Pellegrino, S. E. Bari, D. Bikiel, F. Doctorovich, *J. Am. Chem. Soc.* **2010**, *132*, 989–995.

[18] S. R. Wecksler, A. Mikhailovsky, D. Korystov, P. C. Ford, *J. Am. Chem. Soc.* **2006**, *128*, 3831–3837.

[19] F.-T. Tsai, S.-J. Chiou, M.-C. Tsai, M.-L. Tsai, H.-W. Huang, M.-H. Chiang, W.-F. Liaw, *Inorg. Chem.* **2005**, *44*, 5872–5881.

[20] M.-C. Tsai, F.-T. Tsai, T.-T. Lu, M.-L. Tsai, Y.-C. Wei, I.-J. Hsu, J.-F. Lee, W.-F. Liaw, *Inorg. Chem.* **2009**, *48*, 9579–9591.

[21] a) H. W. Huang, C. C. Tsou, T. S. Kuo, W. F. Liaw, *Inorg. Chem.* **2008**, *47*, 2196–2204; b) Z. J. Tonzetich, L. H. Do, S. J. Lippard, *J. Am. Chem. Soc.* **2009**, *131*, 7964–7965; c) M.-C. Hung, M.-C. Tsai, G.-H. Lee, W.-F. Liaw, *Inorg. Chem.* **2006**, *45*, 6041–6047; d) F.-T. Tsai, T.-S. Kuo, W.-F. Liaw, *J. Am. Chem. Soc.* **2009**, *131*, 3426–3427.

[22] CCDC-759683 (**1**), -759684 (**3**), -759685 (**4**), and -759686 (**5**) contain the supplementary crystallographic data for this paper. These data can be obtained free of charge from The Cambridge Crystallographic Data Centre via www.ccdc.cam.ac.uk/data_request/cif.

[23] R. J. Butcher, E. Sinn, *Inorg. Chem.* **1980**, *19*, 3622–3626.

[24] M. L. Tsai, C. C. Chen, I. J. Hsu, S. C. Ke, C. H. Hsieh, K. A. Chiang, G. H. Lee, Y. Wang, W. F. Liaw, *Inorg. Chem.* **2004**, *43*, 5159–5167.

[25] a) C.-M. Lee, C.-H. Chen, S.-C. Ke, G.-H. Lee, W.-F. Liaw, *J. Am. Chem. Soc.* **2004**, *126*, 8406–8412; b) W.-F. Liaw in *Encyclopedia of Inorganic Chemistry, Ni: Models of Protein Active Sites*, 2nd ed. (Ed.: R. H. Crabtree), Wiley, New York, **2006**; c) C.-H. Chen, G.-H. Lee, W.-F. Liaw, *Inorg. Chem.* **2006**, *45*, 2307–2316.

[26] T.-T. Lu, S.-J. Chiou, C.-Y. Chen, W.-F. Liaw, *Inorg. Chem.* **2006**, *45*, 8799–8806.

[27] a) J. Conradie, D. A. Quarless, Jr., H.-F. Hsu, T. C. Harrop, S. J. Lippard, S. A. Koch, A. Ghosh, *J. Am. Chem. Soc.* **2007**, *129*, 10446–10456; b) C.-M. Lee, C.-H. Chen, H.-W. Chen, J.-L. Hsu, G.-H. Lee, W.-F. Liaw, *Inorg. Chem.* **2005**, *44*, 6670–6679.

[28] A. F. Vanin, A. A. Papina, V. A. Serezhenkov, W. H. Koppenol, *Nitric Oxide* **2004**, *10*, 60–73.

[29] a) M. Feelisch, T. Rassaf, S. Mnaimneh, N. Singh, N. S. Bryan, D. Jourd′heuil, M. Kelm, *FASEB J.* **2002**, *16*, 1775–1785; b) T. Rassaf, N. S. Bryan, M. Kelm, M. Feelisch, *Free Radical Biol. Med.* **2002**, *33*, 1590–1596; c) Y. Y. Zhang, A. M. Xu, M. Nomen, M. Walsh, J. F. Keaney Jr, J. Loscalzo, *J. Biol. Chem.* **1996**, *271*, 14271–14279.

[30] a) L. A. Tyler, J. C. Noveron, M. M. Olmstead, P. K. Mascharak, *Inorg. Chem.* **2000**, *39*, 357–362; b) E. Block, G. Ofori-Okai, J. Zubieta, *J. Am. Chem. Soc.* **1989**, *111*, 2327–2329.

[31] SADABS, Siemens Area Detector Absorption Correction Program, G. M. Sheldrick, University of Göttingen, Göttingen (Germany), **1996**.

[32] SHELXTL, Program for Crystal Structure Determination, G. M. Sheldrick, Siemens Analytical X-ray Instruments Inc., Madison, WI, **1994**.

Received: February 28, 2010
Published online: June 8, 2010

